PROCEEDINGS OF SCIENCE

RG running from Step-Scaling Matrices in χSF schemes for ΔF = 2 Four-Fermion Operators

Isabel Campos Plasencia,[a] **Mattia Dalla Brida,**[b] **Giulia Maria de Divitiis,**[c,d] **Andrew Lytle,**[e] **Riccardo Marinelli,**[f,g,*] **Mauro Papinutto**[f,g] **and Anastassios Vladikas**[d]

[a] *Instituto de Física de Cantabria IFCA-CSIC, Avda. de los Castros s/n, 39005, Santander, Spain*
[b] *Theoretical Physics Department, CERN, CH-1211, Geneva 23, Switzerland*
[c] *Dipartimento di Fisica, Università di Roma "Tor Vergata", Via della Ricerca Scientifica 1, 00133 Roma, Italy*
[d] *INFN, Sezione di Tor Vergata, Via della Ricerca Scientifica 1, 00133 Roma, Italy*
[e] *Department of Physics, University of Illinois at Urbana-Champaign, Urbana, Illinois, 61801, USA*
[f] *Dipartimento di Fisica, Università di Roma La Sapienza, Piazzale A. Moro 2, 00185 Roma, Italy*
[g] *INFN, Sezione di Roma, Piazzale A. Moro 2, 00185 Roma, Italy*

E-mail: isabel.campos@csic.es, mattia.dalla.brida@cern.ch, giulia.dedivitiis@roma2.infn.it, atlytle@illinois.edu, riccardo.marinelli@roma1.infn.it, mauro.papinutto@roma1.infn.it, tassos.vladikas@roma2.infn.it

We present preliminary results for the Renormalization Group (RG) running of the complete basis of $\Delta F = 2$ four-fermion operators in QCD with $N_f = 3$ dynamical massless flavours. We use O(a)-improved Wilson fermions in a mixed action setup, with chirally rotated Schrödinger functional (χSF) boundary conditions for the valence quarks and Schrödinger functional (SF) boundary conditions for the sea quarks. The RG evolution operators are evaluated non-perturbatively via the matrix step-scaling functions (matrix SSF) using a SF coupling from the perturbative region down to $\sim$ 4GeV and a Gradient Flow (GF) coupling from $\sim$ 4GeV down to $\sim$ 250MeV. The perturbative running is computed through a novel approach that extends the usual computations in the literature relying on consequences of the Poincaré-Dulac theorem.

The 41st International Symposium on Lattice Field Theory (LATTICE2024)
28 July - 3 August 2024
Liverpool, UK

*Speaker

PoS(LATTICE2024)286

1. Four-quark operators for $\Delta F = 2$ transitions

The $\Delta F = 2$ transitions, among flavour physics processes, provide some of the most stringent constraints on New Physics (NP) that can be searched in particle accelerators. The existence of new particles can be tested, in fact, looking for their possible effects on low-energy processes. The most general $\Delta F = 2$ weak effective Hamiltonian can be constructed in terms of a complete set of parity even (PE) and parity odd (PO) 4-quark operators, viz.

$$\begin{aligned} \text{PE}: \quad Q_k^{\pm} &\in \left\{ \mathcal{O}^{\pm}_{[VV+AA]}\,,\ \mathcal{O}^{\pm}_{[VV-AA]}\,,\ \mathcal{O}^{\pm}_{[SS-PP]}\,,\ \mathcal{O}^{\pm}_{[SS+PP]}\,,\ 2\mathcal{O}^{\pm}_{[TT]}\cdot \right\}, \\ \text{PO}: \quad \mathcal{Q}_k^{\pm} &\in \left\{ \mathcal{O}^{\pm}_{[VA+AV]}\,,\ \mathcal{O}^{\pm}_{[VA-AV]}\,,\ \mathcal{O}^{\pm}_{[PS-SP]}\,,\ \mathcal{O}^{\pm}_{[PS+SP]}\,,\ -2\mathcal{O}^{\pm}_{[T\tilde{T}]} \right\}, \end{aligned} \tag{1}$$

where we understand $\mathcal{O}^{\pm}_{[\Gamma_1\Gamma_2]} := \frac{1}{2}\left[(\bar{\psi}_1\Gamma_1\psi_2)(\bar{\psi}_3\Gamma_2\psi_4) \pm (\bar{\psi}_1\Gamma_1\psi_4)(\bar{\psi}_3\Gamma_2\psi_2) \right]$.

When considering Wilson-fermions, chiral symmetry is broken by the regularisation, this results in a complicated mixing of the PE operators under renormalisation, while the PO ones still renormalise as in chirally preserving regularizations, namely [1]

$$[\mathcal{Q}_1]_R = \mathcal{Z}_{11}\mathcal{Q}_1, \qquad \begin{bmatrix} \mathcal{Q}_2 \\ \mathcal{Q}_3 \end{bmatrix}_R = \begin{bmatrix} \mathcal{Z}_{22} & \mathcal{Z}_{23} \\ \mathcal{Z}_{32} & \mathcal{Z}_{33} \end{bmatrix} \begin{bmatrix} \mathcal{Q}_2 \\ \mathcal{Q}_3 \end{bmatrix}, \qquad \begin{bmatrix} \mathcal{Q}_4 \\ \mathcal{Q}_5 \end{bmatrix}_R = \begin{bmatrix} \mathcal{Z}_{44} & \mathcal{Z}_{45} \\ \mathcal{Z}_{54} & \mathcal{Z}_{55} \end{bmatrix} \begin{bmatrix} \mathcal{Q}_4 \\ \mathcal{Q}_5 \end{bmatrix}. \tag{2}$$

Using the four-quark operators, the renormalised effective Hamiltonian can be expressed as

$$\mathcal{H}_{\text{eff}} = \frac{G_F}{\sqrt{2}} \sum_i V^i_{CKM} C_i(\mu) O_i(\mu)\,, \tag{3}$$

the coefficients $C_i(\mu)$ are the Wilson coefficients, whose non-perturbative evaluation is shown in this work.

2. Perturbative running for $N_\mathrm{f} = 3$ QCD

In this work we show the procedure followed to evaluate the coefficients C_i whose renormalization is encoded in *evolution operators* that we will call $\hat{\mathbf{U}}(\mu)$. The usual derivation of such operators can be found in [2], but it is not well defined for $N_\mathrm{f} = 3$. The problem has been solved as suggested in [3, 4]: the Poincaré-Dulac theorem guarantees the existence of a basis transformation

$$\bar{\mathcal{Q}}'(x) = \mathbf{S}(g)\bar{\mathcal{Q}}(x)\,, \quad \mathbf{S}(g) = \left(\mathbb{1} + \sum_{k=1}^{\infty} \mathbf{H}_{2k} g^{2k} \right) \mathbf{S}_\mathrm{D} \tag{4}$$

that puts the matrix $\mathbf{A}(g) := \boldsymbol{\gamma}(g)/\beta(g)$ in the so-called *canonical form*, i.e. $\mathbf{A}^{\text{can}}(g) = \frac{1}{g}\left(\boldsymbol{\Lambda} + g^2\mathbf{N}_2\right)$. Here $\boldsymbol{\Lambda}$ is the diagonal matrix of eigenvalues, $\mathbf{N}_2$ is an upper-diagonal matrix, the matrix coefficients $\mathbf{H}_{2k}$ can be obtained recursively, as outlined in ref. [4] and the matrix $\mathbf{S}_\mathrm{D}$ is the one that diagonalises $\boldsymbol{\gamma}(g)/\beta(g)$. In this operator basis, the evolution operator is given by $\hat{\mathbf{U}}_{\text{can}}(\mu) = g(\mu)^{-\boldsymbol{\Lambda}} g(\mu)^{-\mathbf{N}}$ and returning to the original operator basis, we finally get $\hat{\mathbf{U}}(\mu) = \mathbf{S}_\mathrm{D}^{-1}\hat{\mathbf{U}}_{\text{can}}(\mu)\mathbf{S}(\mu)$.

PoS(LATTICE2024)286

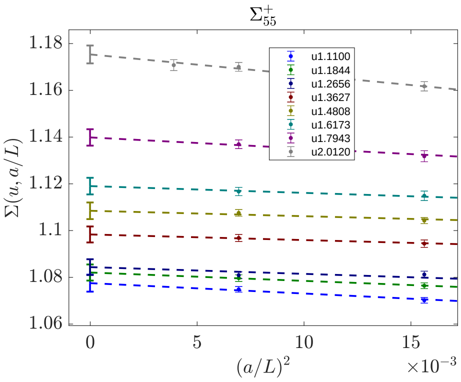

Figure 1: Continuum extrapolation of the matrix element $\left[\tilde{\boldsymbol{\Sigma}}(u, a/L)\right]_{55}$ in the SF region. The extrapolated continuum values $[\boldsymbol{\sigma}(u)]_{55}$ at every coupling, along with their uncertainties, are depicted as a vertical error bar at $a/L = 0$.

3. Non-perturbative running

The non-perturbative part of the operator running is obtained as explained in [5] considering the step-scaling functions (SSFs)

$$\boldsymbol{\sigma}(u) := \mathbf{U}(\mu/2, \mu)\Big|_{\bar{g}^2(\mu)=u} = \lim_{a\to 0} \boldsymbol{\Sigma}\left(g_0^2, a/L\right)\Big|_{\bar{g}^2(1/L)=u} \tag{5}$$

where $\boldsymbol{\Sigma}\left(g_0^2, a/L\right)$ is the discretised step-scaling function that can be obtained from the renormalisation matrices as explained in [6]. The continuum extrapolation on $\boldsymbol{\Sigma}(u, a/L)$ has been performed in two coupling regions, namely SF and GF. In the SF region we analysed data corresponding to the seven couplings $u_{\text{SF}} \in \{1.1844,\ 1.2656,\ 1.3627,\ 1.4808,\ 1.6173,\ 1.7943,\ 2.0120\}$, and to $L/a = 6, 8,\ 12$ (also $L/a = 16$ for $u = 2.0120$) using the ansatz

$$\left[\boldsymbol{\Sigma}\left(u_n, \frac{a}{L}\right)\right]_{ij} = [\boldsymbol{\sigma}(u_n)]_{ij} + \left(\frac{a}{L}\right)^2 \sum_{m=0}^{2} \left[\boldsymbol{\rho}_m\right]_{ij} u_n^m\,, \tag{6}$$

with $n = 1, \ldots, 7$. Moreover, the same global fit has been performed also excluding the $L/a = 6$ data to test the goodness of the latter. The continuum extrapolation in the GF coupling region has been performed simultaneously on data corresponding to the seven couplings $u_{\text{GF}} \in \{2.1257,\ 2.3900,\ 2.7359,\ 3.2029,\ 3.8643,\ 4.4901,\ 5.3013\}$ and to $L/a = 8,\ 12,\ 16$ using the same ansatz in equation (6). The fit parameters have been found minimising the χ^2 function; an example of fit for an SSF matrix element can be found in fig. 1. Obtained the continuum extrapolations at the different couplings available, a functional dependence for $\boldsymbol{\sigma}(u)$ is obtained fitting the latter with two separate fits in the SF and GF regions:

$$\boldsymbol{\sigma}_{\text{SF}}(u) = \mathbf{1} + \mathbf{r}_1 u + \mathbf{r}_2 u^2 + \mathbf{r}_3 u^3 + \mathbf{r}_4 u^4\,, \quad \boldsymbol{\sigma}_{\text{GF}}(u) = \mathbf{R}_0 + \mathbf{R}_1 u + \mathbf{R}_2 u^2\,, \tag{7}$$

where the coefficients $\mathbf{r}_1$ and $\mathbf{r}_2$ are perturbatively defined

$$\mathbf{r}_1 = \boldsymbol{\gamma}_0 \ln 2\,, \quad \mathbf{r}_2 = \boldsymbol{\gamma}_1 \ln 2 + b_0 \boldsymbol{\gamma}_0 \ln^2 2 + \frac{1}{2}(\boldsymbol{\gamma}_0)^2 \ln^2 2\,, \tag{8}$$

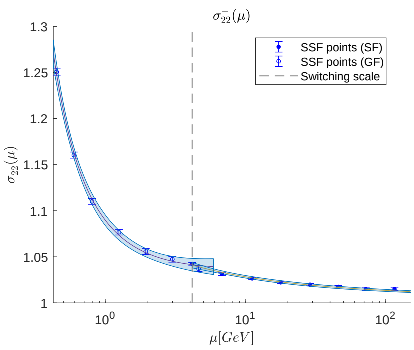

Figure 2: Example of step-scaling function fits. The solid points represent the continuum extrapolations of the step-scaling function in the SF region, while the hollow points represent the extrapolations in the GF region. As can be seen, the fit functions obtained in the GF and SF regions connect at the switching scale (grey dashed line) when expressed as functions of the renormalization scale.

provided that the matrix $\boldsymbol{\gamma}_1$ is evaluated in the SF scheme, this has been done as suggested in [2]. A series of N squared-couplings $u_1 \dots u_{\rm N}$ is then generated through the coupling step-scaling function [7], i.e. evaluating $u_n = \sigma^{-1}(u_{n-1})$, in order to compute non-perturbatively the quantity

$$\mathbf{U}(\mu_{\rm had} \equiv \mu_1, \mu_{\rm pt} \equiv \mu_N) = \boldsymbol{\sigma}(\mu_1) \cdots \boldsymbol{\sigma}(\mu_N)\,, \quad \boldsymbol{\sigma}(\mu) = \boldsymbol{\sigma}(u(\mu)). \tag{9}$$

4. Matching between SF and GF schemes

The results of the fits for the step-scaling functions provide an important test for the reliability of our data, since the step-scaling functions $\sigma(\mu)$ should be continuous; therefore, we expect the fits performed in the SF and GF regions to connect at the switching scale. This expectation has generally been met, both when considering the data with $L/a = 6$ and when excluding them. An example of a step-scaling function fit, represented as a function of the variable μ, can be seen in fig. 2.

5. Results

Using the factorisation properties of the evolution operators [2], we get the non perturbative determination for the one-scale RG evolution operator as function of the coupling:

$$\hat{\mathbf{U}}(\mu) = \mathbf{S}_{\rm D}^{-1} u(\mu_{\rm pt})^{-\boldsymbol{\Lambda}/2} u(\mu_{\rm pt})^{-\mathbf{N}_2/2} \Big(\mathbb{1} + u(\mu_{\rm pt})\mathbf{H}_2 + u^2(\mu_{\rm pt})\mathbf{H}_4 + u^3(\mu_{\rm pt})\mathbf{H}_6\Big) \mathbf{S}_{\rm D} \mathbf{U}(\mu_{\rm pt}, \mu) \tag{10}$$

and μ is related to u in the SF region through the relation [7]

$$\frac{\mu}{\Lambda} = (b_0 u)^{\frac{b_1}{2b_0^2}} \exp\left(\frac{1}{2b_0 u}\right) \exp\left[\int_0^{\sqrt{u}} \mathrm{d}x \left(\frac{1}{\beta(x)} + \frac{1}{b_0 x^3} - \frac{b_1}{b_0^2 x}\right)\right], \tag{11}$$

where Λ is computed in the SF scheme in [8]. In the GF region, μ is computed using [9] the parametrisation

$$\beta_{\rm GF} = -u^{3/2}/(p_0 + p_1 u + p_2 u^2)\,, \tag{12}$$

with $p_0 = 16.63 \pm 0.61$, $p_1 = -0.05 \pm 0.20$, $p_2 = 0.008 \pm 0.016$.

We associated two kinds of uncertainties to the running that we computed:

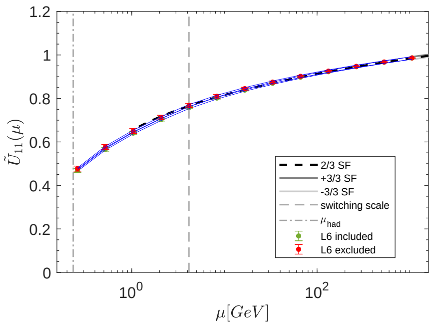

Figure 3: Non-perturbative running $\hat{U}_{11}(\mu)$ (red and green points, $N = 9$) compared to the NLO prediction (black dashed curve). The red points refer to fits evaluated excluding the $L/a = 6$ data, while the green ones are obtained taking into account $L/a = 6$ data too. The curves in blue are built evolving non-perturbatively the $\pm(3/3)$SF runnings and quantify the systematic error.

- statistical error computed propagating the error on $\boldsymbol{\sigma}(u)$ in the formula (9),
- systematic error due to the lack of knowledge of the NNLO matrix $\boldsymbol{\gamma}_2$.

The systematic error has been evaluated as follows. Having no theoretical hint on the entity of $\boldsymbol{\gamma}_2$, we only consider two guesstimates: $\boldsymbol{\gamma}_2^{\mathrm{L}} = -\boldsymbol{\gamma}_1/4$, $\boldsymbol{\gamma}_2^{\mathrm{R}} = \boldsymbol{\gamma}_1/4$, whose rough choice will be enlightened after the results for the running are shown. Using the guesses for $\boldsymbol{\gamma}_2$ we evaluated guesstimates of the matrices $\mathbf{H}_4^{\mathrm{L/R}}$, $\mathbf{H}_6^{\mathrm{L/R}}$ and consequently the guessed perturbative RG evolution $\hat{\mathbf{U}}^{\mathrm{L/R}}(u_{\mathrm{pt}})$ that we will address as $\mp\mathbf{(3/3)SF}$. We were then able to evaluate the guessed non-perturbative running as defined in (10), where we imposed the matching at the same scale used for the (2/3)SF results. Eventually, we defined the systematic error as the difference between the non-perturbative running (2/3)SF and the guessed runnings $\mp(3/3)$SF.

The number of steps $N = 9$ resulted in limited statistical uncertainties and negligible systematic ones, therefore we opted to produce plots for $N = 9$. The latter can be found in fig.s (3), (4) and (5), where the non-perturbative running points are compared to the perturbative (2/3)SF running and both statistical and systematic uncertainties are separately displayed.

6. Conclusions

In this work, we provided a non-perturbative renormalization of the four-fermion operators introduced in eq. (1) investigating the RG running and mixing of the operator basis in a $N_{\mathrm{f}} = 3$ QCD between a low-energy scale $\mu_{\mathrm{had}} \sim \mathcal{O}(250)$MeV and a high-energy scale $\mu_{\mathrm{pt}} \sim \mathcal{O}(10^3)$GeV, where we used a GF coupling between the hadronic scale and $\sim$ 4GeV and a SF coupling afterwards. We included the NLO anomalous dimension matrix $\boldsymbol{\gamma}_1$ in the computation for the perturbative part of the evolution operator $\tilde{\mathbf{U}}(\mu)$ and generalized its definition.

Our analysis introduced two kinds of uncertainties: statistical and systematic. The statistical uncertainties have been evaluated through the bootstrap analysis of the simulated data and have been propagated in the various computations. The systematic uncertainties have been introduced to estimate the possible effect on our results that may be introduced by the unknown NNLO anomalous

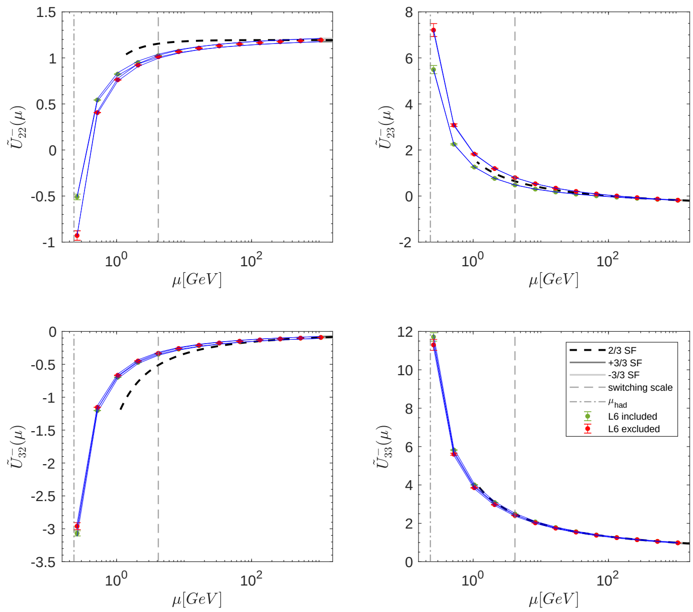

Figure 4: Non-perturbative running for the matrix elements 2|3 of the evolution operator $\hat{\mathbf{U}}(\mu)$ (green and red points, $N = 9$). The results are compared to the NLO prediction (black curve). The curves in blue are built evolving non-perturbatively the $\pm(3/3)$SF runnings and quantify the systematic error.

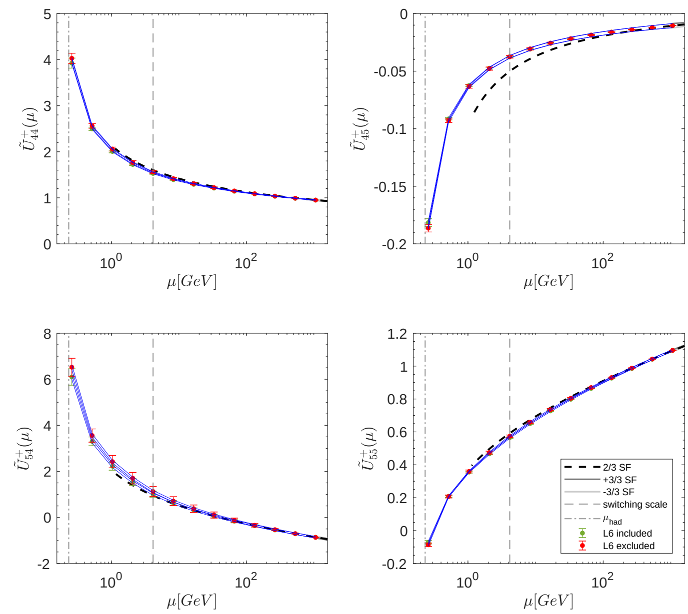

Figure 5: Non-perturbative running for the matrix elements 4|5 of the evolution operator $\hat{\mathbf{U}}(\mu)$ (green and red points, $N = 9$). The results are compared to the NLO prediction (black curve). The curves in blue are built evolving non-perturbatively the $\pm(3/3)$SF runnings and quantify the systematic error.

dimension matrix $\boldsymbol{\gamma}_2$, they can be made negligible if the matching scale is large enough and, as for the current knowledge, we can give only guesses of these errors.

We represented the non-vanishing matrix elements of $\hat{\mathbf{U}}$ in fig.s 3, 4 and 5, where it is possible to notice that the points corresponding to the non-perturbative evaluations approach the perturbative running with the same slope and distinguish from the perturbation theory at the lower energy scales.

The results presented highlight the limitations (at least for the renormalisation scheme considered) of perturbation theory at scales around $O(1)$ GeV, as evidenced by the behaviour of the matrix elements $\hat{U}_{22}$, $\hat{U}_{32}$, and $\hat{U}_{45}$. The non-perturbative approaches employed here are shown to be essential for the reliable renormalization of the FFO, particularly at low-energy scales. Future efforts may aim to further reduce systematic uncertainties and explore higher-order corrections to enhance the precision of the renormalization group analysis.

References

[1] A. Donini, V. Gimenez, G. Martinelli, M. Talevi and A. Vladikas, *Nonperturbative renormalization of lattice four fermion operators without power subtractions*, *Eur. Phys. J. C* **10** (1999) 121 [hep-lat/9902030].

[2] M. Papinutto, C. Pena and D. Preti, *On the perturbative renormalization of four-quark operators for new physics*, *Eur. Phys. J. C* **77** (2017) 376 [1612.06461].

[3] M. Becchetti and M. Bochicchio, *Operator mixing in massless QCD-like theories and Poincarè–Dulac theorem*, *Eur. Phys. J. C* **82** (2022) 866 [2103.16220].

[4] M. Bochicchio, *On the geometry of operator mixing in massless QCD-like theories*, *Eur. Phys. J. C* **81** (2021) 749 [2103.15527].

[5] ALPHA collaboration, P. Dimopoulos, G. Herdoíza, M. Papinutto, C. Pena, D. Preti and A. Vladikas, *Non-Perturbative Renormalisation and Running of BSM Four-Quark Operators in $N_f = 2$ QCD*, *Eur. Phys. J. C* **78** (2018) 579 [1801.09455].

[6] I. Campos Plasencia, M. Dalla Brida, G. de Divitiis, A. Lytle, R. Marinelli, M. Papinutto et al., *Non-perturbative mixing and renormalisation of ΔF=2 Four-Fermion Operators*, *PoS* **LATTICE2023** (2024) 270.

[7] ALPHA collaboration, M. Dalla Brida, P. Fritzsch, T. Korzec, A. Ramos, S. Sint and R. Sommer, *A non-perturbative exploration of the high energy regime in $N_f = 3$ QCD*, *Eur. Phys. J. C* **78** (2018) 372 [1803.10230].

[8] ALPHA collaboration, M. Bruno, M. Dalla Brida, P. Fritzsch, T. Korzec, A. Ramos, S. Schaefer et al., *QCD Coupling from a Nonperturbative Determination of the Three-Flavor Λ Parameter*, *Phys. Rev. Lett.* **119** (2017) 102001 [1706.03821].

[9] ALPHA collaboration, I. Campos Plasencia, M. Dalla Brida, G. de Divitiis, A. Lytle, M. Papinutto, L. Pirelli et al., *Nonperturbative running of the tensor operator for $N_f = 3$ QCD from the chirally rotated Schrödinger functional*, *Phys. Rev. D* **109** (2024) 054511 [2311.15046].